Letter | Editors' Suggestion

Mott transition from the nonanalyticity of the one-body reduced density-matrix functional

Zhengqian Cheng and Chris A. Marianetti
Department of Applied Physics and Applied Mathematics, Columbia University, New York, New York 10027, USA

(Received 18 August 2025; revised 19 January 2026; accepted 27 January 2026; published 20 February 2026)

One-body reduced density-matrix functional (1RDMF) theory has yielded promising results for small systems such as molecules, but has not addressed quantum phase transitions such as the Mott transition. Here we explicitly execute the constrained search within a variational ansatz to construct a 1RDMF for the multiorbital Hubbard model with up to seven orbitals in the thermodynamic limit. The variational ansatz is the $\mathcal{N}=3$ ansatz of the variational discrete action theory (VDAT), which can be exactly evaluated in $d=\infty$. The resulting 1RDMF exactly encapsulates the $\mathcal{N}=3$ VDAT results, which accurately captures Mott and Hund physics. We find that nonanalytic behavior emerges in our 1RDMF at fixed integer filling, which gives rise to the Mott transition. We explain this behavior by separating the constrained search into multiple stages, illustrating how a nonzero Hund exchange drives the continuous Mott transition to become first-order. Our approach creates a new path forward for constructing an accurate 1RDMF for strongly correlated electron materials.

DOI: 10.1103/z7qw-99jc

One-body reduced density-matrix functional (1RDMF) theory can be viewed as a formalism to encapsulate the ground-state properties for a class of Hamiltonians with fixed interactions and arbitrary one-body terms [1–6]. While the existence of the exact 1RDMF can be proven using the constrained search, the 1RDMF is only useful if reliable approximations can be developed. An analogous scenario can be found in density functional theory, where the formally exact exchange-correlation functional can be approximated using the local density approximation [7]. The breakthrough in the present work is demonstrating that the 1RDMF can be constructed by exactly executing the constrained search within a nontrivial variational ansatz for the multiorbital Hubbard model in $d=\infty$.

There have been successes in developing explicit 1RDMF's which produce reasonable energetics in various molecules [4,8–14] and single orbital Hubbard models [15–27], in addition to select observables in crystals [28–32]. However, there has not been a rigorous demonstration that any existing 1RDMF can capture the Mott transition. Our focus is capturing local Mott and Hund physics, which is hosted in strongly correlated electron materials (SCEM) which often bear d or f electrons [33]. The essence of SCEM is embodied by the multiorbital Hubbard model in infinite dimensions, which facilitates numerically exact solutions and serves as a reasonable starting approximation for crystals in two and three dimensions [33–36]. While the dynamical mean-field theory (DMFT) is the *de facto* standard for computing the Green's function of the $d=\infty$ Hubbard model, the variational discrete action theory (VDAT) [37,38] offers an alternate route to the exact ground-state properties within the variational paradigm. In this paper, we demonstrate that VDAT is an essential tool for constructing a robust 1RDMF for the $d=\infty$ Hubbard model.

A robust 1RDMF of the multiorbital Hubbard model should satisfy the following criteria, which are dictated by numerically exact solutions in infinite dimensions. First, the Mott transition must be predicted at a finite Hubbard U. Second, the order of the Mott transition must be properly predicted with or without the Hund coupling J. Third, the aforementioned goals should be achieved while maintaining the symmetry of the Hamiltonian, proving that the functional can faithfully describe Mott and Hund physics. Here we demonstrate that an accurate 1RDMF that satisfies the preceding criteria can be constructed by *exactly* executing the constrained search within the $\mathcal{N}=3$ sequential product density-matrix (SPD) ansatz of VDAT in infinite dimensions [37,38]. Given that VDAT at $\mathcal{N}=3$ has been demonstrated to accurately capture Mott and Hund physics [39,40], the resulting 1RDMF serves as an efficient approach to exactly encapsulate VDAT results. A companion article to this Letter introduces the qubit parametrization of VDAT, which provides the technical tools needed to execute the constrained search [41].

For simplicity, we consider the translationally invariant Hamiltonian $\hat{H}=\sum_{k\ell}\epsilon_{k\ell}\hat{n}_{k\ell}+\hat{H}_{\rm int}$, where k labels a reciprocal lattice point, ℓ enumerates $2N_{\rm orb}$ spin orbitals, and the interaction Hamiltonian is $\hat{H}_{\rm int}=\sum_i H_{\rm loc}(\{\hat{n}_{i\ell}\})$ where $H_{\rm loc}$ is an arbitrary polynomial function and $\hat{n}_{i\ell}$ is the density operator for spin orbital ℓ at site i. It should be noted that the one-body contribution is restricted to be diagonal in ℓ and the local interactions are restricted to a density-density form, which are common simplifications used when studying the multiorbital Hubbard model (e.g., see Ref. [42]). For this class of Hamiltonians, the interaction energy functional is defined as

$$E_{\rm int}(\{n_{k\ell}\})=\frac{1}{L}\min_{|\Psi\rangle}\{\langle\Psi|\hat{H}_{\rm int}|\Psi\rangle\big|\langle\Psi|\hat{n}_{k\ell}|\Psi\rangle=n_{k\ell}\},\qquad(1)$$

where $|\Psi\rangle$ is a normalized state in the many-particle Fock space, L is the number of sites in the lattice, and $n_{k\ell}\in[0,1]$. For a given $\hat{H}_{\rm int}$, the interaction functional $E_{\rm int}$ is universal in the sense that it provides the ground-state energy for

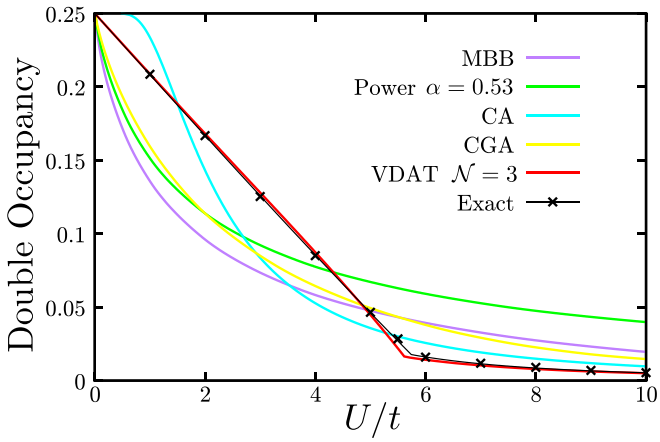

FIG. 1. Double occupancy vs U/t for the single-orbital Hubbard model on the Bethe lattice in $d=\infty$ using four 1RDMF's: MBB, Power, CA, and CGA. The exact DMFT and VDAT results are taken from Ref. [38]. The black line is obtained from interpolations of the metallic and insulating DMFT data. The 1RDMF derived in the present work exactly reproduces the VDAT results (red line).

Hamiltonians with arbitrary $\epsilon_{k\ell}$ as follows:

$$E=\min_{\{n_{k\ell}\}}\left(\frac{1}{L}\sum_{k\ell}\epsilon_{k\ell}n_{k\ell}+E_{\rm int}(\{n_{k\ell}\})\right). \tag{2}$$

While $E_{\rm int}(\{n_{k\ell}\})$ must be explicitly constructed for a given $\hat{H}_{\rm int}$, the interacting energy functional for $\lambda\hat{H}_{\rm int}$, where λ is a positive number, is the interacting energy functional for $\hat{H}_{\rm int}$ multiplied by λ.

We begin by examining the fidelity of numerous explicit 1RDMF's from the literature by applying them to the single-orbital Hubbard model in $d=\infty$, including the MBB [43], CA [44], CGA [45], and power [30] functionals, all of which approximate the interaction energy functional as a Hartree term plus an exchange-correlation term which consists of independent contributions from each spin orbital. We compare all functionals to numerically exact solutions obtained using DMFT [34,36] with the numerical renormalization group impurity solver [46], in addition to VDAT results for $\mathcal{N}=3$ [38] (see Fig. 1). The VDAT results correctly describe the continuous Mott transition [34], identified by a kink in the double occupancy at $U/t=5.61784$, and accurately agree with the DMFT results. These VDAT results will be exactly reproduced by the 1RDMF derived in the present work. The MBB, CA, CGA, and power functionals are all substantially in error, and qualitatively fail to predict the Mott transition at a finite U/t. More advanced functionals, including PNOF5 [12] and PNOF7 [47], also perform poorly in the absence of symmetry breaking [41].

Our proposed solution for obtaining the interaction energy functional is to rigorously execute the constrained search within the SPD ansatz [37,38], which is the ansatz used in VDAT. The variational freedom of the SPD is set by an integer $\mathcal{N}$, where $\mathcal{N}\to\infty$ encapsulates the exact solution, and there are two types of SPD: G-type or B-type. A restricted form of the SPD has been evaluated using quantum Monte-Carlo to solve the single-orbital Hubbard model in two dimensions [48–53], the p-d model [54,55], and selected molecules [56]. Alternatively, VDAT has been used to exactly evaluate the SPD in the Anderson impurity model [38], the single orbital Hubbard model in $d=\infty$ [38], and the multiorbital Hubbard model in $d=\infty$ [39,40]. Nonetheless, constructing $E_{\rm int}(\{n_{k\ell}\})$ from any nontrivial variational ansatz is still highly challenging as there must be some efficient means to constrain the variational parameters to a particular $\{n_{k\ell}\}$ and minimize over the remaining degrees of freedom. The recently developed qubit parametrization of VDAT allows for the constrained search to be executed for the B-type $\mathcal{N}=2$ and the G-type $\mathcal{N}=2$ and $\mathcal{N}=3$ SPD, and here we focus on G-type $\mathcal{N}=3$ (see Ref. [41] for $\mathcal{N}=2$).

We now proceed to construct the interaction energy functional via the $\mathcal{N}=3$ G-type SPD, and it is sufficient to restrict the SPD to a pure state which can be represented as

$$|\Psi\rangle=\exp\left(\sum_{k\ell}\gamma_{k\ell}\hat{n}_{k\ell}\right)\exp\left(\sum_{i\Gamma}\upsilon_{\Gamma}\hat{X}_{i\Gamma}\right)|\Psi_0\rangle, \tag{3}$$

where $|\Psi_0\rangle$ is a Slater determinant, $\hat{X}_{i\Gamma}$ is a diagonal Hubbard operator at site i, and the variational parameters are $\{\gamma_{k\ell}\}$, $\{\upsilon_{\Gamma}\}$, and $\{n_{k\ell;0}\}$, where $n_{k\ell;0}=\langle\Psi_0|\hat{n}_{k\ell}|\Psi_0\rangle\in\{0,1\}$. The index Γ enumerates all $2^{2N_{\rm orb}}$ local atomic states. The key idea is to reparametrize the variational parameters $\{\gamma_{k\ell}\}$ and $\{\upsilon_{\Gamma}\}$ from Eq. (3) in terms of new variational parameters $\{n_{k\ell}\}$ and $\boldsymbol{\rho}$. The $\{n_{k\ell}\}$ is the physical momentum density distribution taking values within [0,1], and has the same number of free parameters as $\{\gamma_{k\ell}\}$. The $\boldsymbol{\rho}$ is a many-body density matrix corresponding to a pure state of a $2N_{\rm orb}$ qubit system, which has the same number of independent parameters as $\{\upsilon_{\Gamma}\}$. The qubit system is a convenient mathematical tool to represent local integer time correlation functions of the VDAT formalism as static observables [41]. There is a natural correspondence between the density operators in the local Fock space and the qubit space, where the local density operator is represented as $\hat{n}_{\ell}=\frac{1}{2}(1-\hat{\sigma}_{\ell}^{z})$, and $\hat{\sigma}_{\ell}^{\mu}$ denotes the application of the $\hat{\sigma}^{\mu}$ Pauli matrix to the ℓth qubit subspace. Using these new variables, the interaction energy for a given set of variational parameters can be expressed as $\langle\hat{H}_{\rm eff}\rangle_{\boldsymbol{\rho}}$, where $\hat{H}_{\rm eff}=H_{\rm loc}(\{\hat{n}_{{\rm eff},\ell}\})$ is defined in the qubit space, and $\hat{n}_{{\rm eff},\ell}$ depends on the variational parameters only through the following five variables: $n_{\ell}=\int dk n_{k\ell}$, $\xi_{\ell}=\frac{1}{2}\langle\hat{\sigma}_{\ell}^{x}\rangle_{\boldsymbol{\rho}}$, $\Delta_{\ell}=\int_{>}dk n_{k\ell}$, and $\mathcal{A}_{X\ell}=\int_{X}dk\sqrt{n_{k\ell}(1-n_{k\ell})}$, where X takes two values denoted as $<$ or $>$ indicating that the integration is over the region where $n_{k\ell,0}=1$ or $n_{k\ell,0}=0$ for a given ℓ, respectively. Here we have taken the continuum limit of the discretized $n_{k\ell}$ and choose the convention $\int dk=1$. It should be emphasized that $\hat{n}_{{\rm eff},\ell}$ *analytically* depends on the preceding five variables (see Eq. (68) in Ref. [41]). Finally, the interaction energy functional can be conveniently expressed as a constrained minimization

$$E_{\rm int}(\{n_{k\ell}\})=\min_{\boldsymbol{\rho},\{n_{k\ell;0}\}}\langle\hat{H}_{\rm eff}\rangle_{\boldsymbol{\rho}}, \tag{4}$$

$$\text{subject to}\quad\int dk n_{k\ell;0}=\left\langle\frac{1-\hat{\sigma}_{\ell}^{z}}{2}\right\rangle_{\boldsymbol{\rho}}=\int dk n_{k\ell}, \tag{5}$$

$$\left|\langle\hat{\sigma}_{\ell}^{x}\rangle_{\boldsymbol{\rho}}\right|\leqslant 2\sqrt{(1-n_{\ell})n_{\ell}-(1-\Delta_{\ell})\Delta_{\ell}}, \tag{6}$$

which corresponds to an *exact* constrained search within the wave function given by Eq. (3) in $d=\infty$. We assume that

the optimized $n_{k\ell;0}$ is given as $\theta(n_{k\ell} - n_\ell^\star)$, where θ is the Heaviside function and $n_\ell^\star$ is chosen such that $\int dk n_{k\ell;0} = n_\ell$. The remaining challenge is how to efficiently minimize $\langle \hat{H}_{\text{eff}} \rangle_{\boldsymbol{\rho}}$ over $\boldsymbol{\rho}$, which is nontrivial given that $\hat{H}_{\text{eff}}$ depends on $\boldsymbol{\rho}$ through ξ_ℓ. This challenge can be addressed by dividing the minimization into two stages. First, $\{\xi_\ell\}$ can be fixed, which will fix $\hat{H}_{\text{eff}}$, and then $\langle \hat{H}_{\text{eff}} \rangle_{\boldsymbol{\rho}}$ can be minimized, which is equivalent to finding the ground state of $\hat{H}_{\text{eff}} - \sum_\ell h_\ell^x \hat{\sigma}_\ell^x - \sum_\ell h_\ell^z \hat{\sigma}_\ell^z$, where the Lagrange multipliers h_ℓ^μ are chosen to yield $\langle \hat{\sigma}_\ell^x \rangle_{\boldsymbol{\rho}} = 2\xi_\ell$ and $\langle \hat{\sigma}_\ell^z \rangle_{\boldsymbol{\rho}} = 1 - 2n_\ell$. Second, the interaction energy functional is obtained by minimizing over $\{\xi_\ell\}$. In what follows, we will illustrate this two stage minimization for the case where $n_{k\ell}$ is restricted to be independent of ℓ and have particle-hole symmetry, which is sufficient to solve a multiorbital Hubbard model where $\epsilon_{k\ell}$ is independent of ℓ and has particle-hole symmetry.

We consider the following multiorbital interaction Hamiltonian $H_{\text{loc}}(\{\hat{n}_\ell\}) = U\hat{O}$, where

$$\hat{O} = \hat{O}_1 + \left(1 - 2\frac{J}{U}\right)\hat{O}_2 + \left(1 - 3\frac{J}{U}\right)\hat{O}_3, \tag{7}$$

where $\hat{O}_1 = \sum_\alpha \delta\hat{n}_{\alpha\uparrow}\delta\hat{n}_{\alpha\downarrow}$, $\hat{O}_2 = \sum_{\alpha<\beta,\sigma} \delta\hat{n}_{\alpha\sigma}\delta\hat{n}_{\beta\bar{\sigma}}$, $\hat{O}_3 = \sum_{\alpha<\beta,\sigma} \delta\hat{n}_{\alpha\sigma}\delta\hat{n}_{\beta\sigma}$, and $\delta\hat{n}_{\alpha\sigma} = \hat{n}_{\alpha\sigma} - \frac{1}{2}$, with the orbital indices α, β taking values of $1, \ldots, N_{\text{orb}}$ and the spin index $\sigma \in \{\uparrow, \downarrow\}$. The restriction of particle-hole symmetry at half-filling ensures that $\mathcal{A}_{<\ell} = \mathcal{A}_{>\ell}$ and $n_\ell = \frac{1}{2}$, and for convenience we define $A = \mathcal{A}_{<\ell} + \mathcal{A}_{>\ell}$ and also discard the index ℓ for ξ_ℓ and Δ_ℓ. The interaction energy functional implicitly depends on N_{orb}, U, and J, but scaling the interaction Hamiltonian will trivially scale the interaction energy functional. Therefore, the interaction energy functional only has a nontrivial dependence on N_{orb} and J/U.

The interaction energy per site can be written as $\langle \hat{H}_{\text{eff}} \rangle_{\boldsymbol{\rho}} = UA^4 \tilde{\mathcal{F}}^2(\Delta, \xi)\langle \hat{O} \rangle_{\boldsymbol{\rho}}$ (see Eq. (431) in Ref. [41]), where

$$\tilde{\mathcal{F}}(\Delta, \xi) = \frac{2}{1 - 4\xi^2}\left(\sqrt{1 - \frac{4\xi^2}{(1 - 2\Delta)^2}} + 1\right). \tag{8}$$

Following the two stage minimization outlined above, we first minimize the interaction energy over $\boldsymbol{\rho}$ under a constrained value of ξ by computing

$$\mathcal{O}(\xi) = \min_{\boldsymbol{\rho}} \left\{ \langle \hat{O} \rangle_{\boldsymbol{\rho}} \middle| \frac{1}{2}\langle \hat{\sigma}_\ell^x \rangle_{\boldsymbol{\rho}} = \xi, \langle \hat{\sigma}_\ell^z \rangle_{\boldsymbol{\rho}} = 0 \right\}, \tag{9}$$

which encodes the essential information about all local correlations. The computational cost for evaluating $\mathcal{O}(\xi)$ will generally scale exponentially in terms of N_{orb}, but it will be demonstrated that only a coarse disctretization in ξ is needed to faithfully represent $\mathcal{O}(\xi)$. A given data point can be generated efficiently by solving the ground-state of $\hat{O} - h\sum_\ell \hat{\sigma}_\ell^x$, where h is a Lagrange multiplier, which is a transverse field Ising model. In Fig. 2, $\mathcal{O}(\xi)$ is plotted for $N_{\text{orb}} = 2$ and various J/U, demonstrating that the result is indeed a smooth function which can be accurately represented by a spline interpolation. Given that $\mathcal{O}(\xi)$ is demonstrated to be an analytic function when $|\xi| < \frac{1}{2}$, any nonanalytic behavior in the interaction energy must arise from minimizing over ξ. The interaction

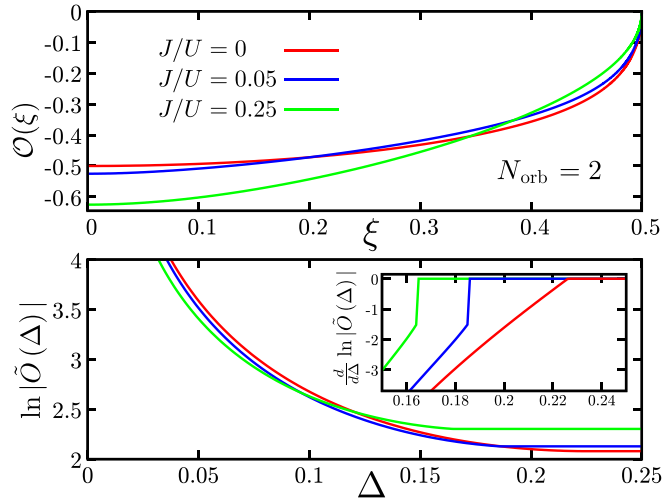

FIG. 2. Plots of $\mathcal{O}(\xi)$ (top) and $\ln|\tilde{O}(\Delta)|$ (bottom) for $N_{\text{orb}} = 2$ and various J/U; the inset plots $\frac{d}{d\Delta}\ln|\tilde{O}(\Delta)|$, highlighting the nonanalytic behavior in the 1RDMF.

energy functional can be *explicitly* constructed when $n_{k\ell}$ is independent of ℓ and has particle hole symmetry, given as

$$E_{\text{int}}(\{n_{k\ell}\}) = UA^4\tilde{O}(\Delta), \tag{10}$$

$$\tilde{O}(\Delta) = \min_{\xi\in[0,\frac{1}{2}-\Delta]} \tilde{\mathcal{F}}^2(\Delta, \xi)\mathcal{O}(\xi), \tag{11}$$

where $\tilde{O}(\Delta)$ can be efficiently evaluated using the spline of $\mathcal{O}(\xi)$, and the result can be accurately represented with a spline interpolation as well. Moreover, for the case of $N_{\text{orb}} = 1$, an analytical form of $\tilde{O}(\Delta)$ can be derived (see Eq. (103) in Ref. [41]). Given that $\tilde{O}(\Delta)$ is constructed for a given J/U and N_{orb}, the result may be used to solve any model with $\epsilon_{k\ell}$ independent of ℓ with particle-hole symmetry and U. In Fig. 2, we plot $\ln|\tilde{O}(\Delta)|$ and $d\ln|\tilde{O}(\Delta)|/d\Delta$ for $N_{\text{orb}} = 2$ and various J/U, demonstrating that there is a discontinuity at $\Delta = \Delta_c$ in the first derivative for $J/U > 0$ and the second derivative for $J/U = 0$. The presence of nonanalyticity in the interaction energy functional is profound, as it guarantees that there must be a phase transition for an arbitrary band structure at some critical U, and this transition will be demonstrated to be the Mott transition. This nonanalytic behavior in the interaction energy functional should not be confused with the derivative discontinuity in density functional theory [57], which is associated with a change in the total number of particles and is present for all systems with a charge gap.

We now explore why $E_{\text{int}}(\{n_{k\ell}\})$ has nonanalytic regions by investigating the minimization over ξ. Consider the function $\mathcal{L}(\Delta, \xi) = -\frac{\tilde{\mathcal{F}}^2(\Delta,\xi)\mathcal{O}(\xi)}{\tilde{\mathcal{F}}^2(\Delta,0)\mathcal{O}(0)}$, where $\mathcal{L}(\Delta, 0) = -1$. Finding the minimum of $\mathcal{L}(\Delta, \xi)$ will yield the minimum of $\tilde{\mathcal{F}}^2(\Delta, \xi)\mathcal{O}(\xi)$ used in Eq. (11), given that $\tilde{\mathcal{F}}(\Delta, 0) = 4$ and $\mathcal{O}(0) = -\frac{1}{4}N_{\text{orb}}(1 + (N_{\text{orb}} - 1)J/U)$. We first consider $J/U = 0$ at $N_{\text{orb}} = 2$ for various Δ (see Fig. 3), demonstrating that the optimized ξ will continuously go to zero as Δ increases through Δ_c. Alternatively, for $J/U > 0$, the optimized ξ will discontinuously go to zero as Δ increases through Δ_c. Therefore, in both cases, $\Delta > \Delta_c$ indicates $\xi = 0$ and $\frac{d\tilde{O}(\Delta)}{d\Delta} = 0$ [see Eq. (8)], which can be seen in Fig. 2. A

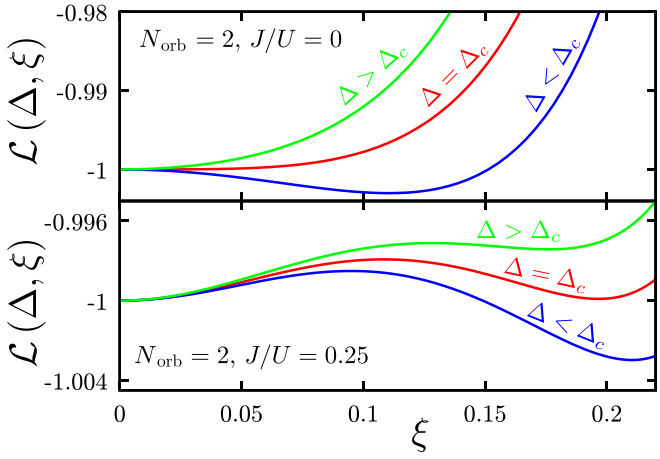

FIG. 3. Graphical illustration of the origin of the nonanalyticity in the interacting energy functional. Plots of $\mathcal{L}(\Delta, \xi)$ vs ξ at $N_{\rm orb} = 2$ with $J/U = 0$ (top) and $J/U = 0.25$ (bottom) for various Δ, where Δ_c corresponds to the nonanalytical point in $\tilde{O}(\Delta)$.

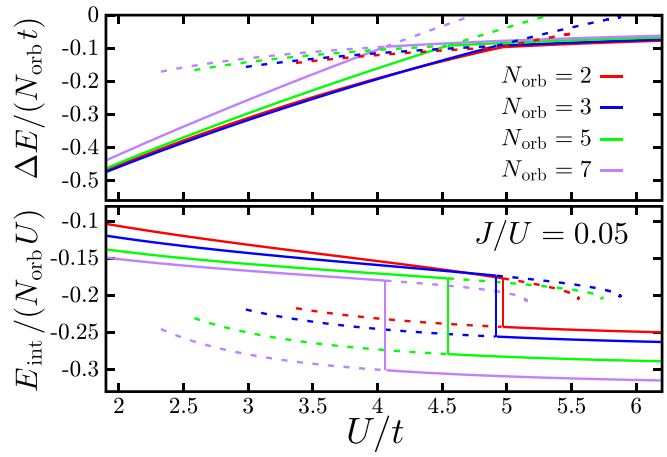

FIG. 4. Plots of various energy contributions for the multiorbital Hubbard model on the Bethe lattice in $d = \infty$ for $N_{\rm orb} = 2, 3, 5, 7$ as a function of U/t for $J/U = 0.05$. (Top) Plot of $\Delta E/(N_{\rm orb}t)$, where $\Delta E = E(U, J, t) - E(U, J, 0)$ and $E(U, J, t)$ is the total energy per site. (Bottom) Plot of $E_{\rm int}/(N_{\rm orb}U)$. The dotted lines indicate metastable solutions.

sixth-order Taylor series expansion of $\mathcal{L}(\Delta, \xi)$ in terms of ξ can be used to provide an analytical understanding of the nonanalyticity in $\tilde{O}(\Delta)$ (see Sec. VII C in Ref. [41]).

We now demonstrate that $\frac{d\tilde{O}(\Delta)}{d\Delta} = 0$ indicates that the system is in the Mott phase. Given that the interaction energy only depends on $\{n_{k\ell}\}$ via Δ and A, the total energy can be partially optimized for a fixed Δ and A, which is achieved by the following momentum density distribution [40,41]

$$n_{k\ell} = \frac{1}{2}\left(1 - \frac{\mathrm{sgn}(\epsilon_{k\ell})a + \epsilon_{k\ell}}{\sqrt{(\mathrm{sgn}(\epsilon_{k\ell})a + \epsilon_{k\ell})^2 + b^2}}\right), \qquad (12)$$

where a and b are Lagrange multipliers that are determined by Δ and A. The partially optimized energy is a function of Δ and A, and rewriting the saddle point equations yields $a = \frac{UA^4}{4N_{\rm orb}}\frac{d\tilde{O}(\Delta)}{d\Delta}$ and $b = \frac{-2UA^3}{N_{\rm orb}}\tilde{O}(\Delta)$ (see Eqs. (483) and (484) in Ref. [41]). Given that the quasiparticle weight $Z = a/\sqrt{a^2 + b^2}$, and that $A > 0$ for finite U, the only scenario where $Z = 0$ is when $\frac{d\tilde{O}(\Delta)}{d\Delta} = 0$. Determining the order of the phase transition requires a global comparison of the total energy between the metal and insulating phases, and the transition only occurs at Δ_c when the transition is continuous (see Sec. VII C in Ref. [41]).

We now proceed to use the 1RDMF to solve the multiorbital Hubbard model on the Bethe lattice in $d = \infty$ for $N_{\rm orb} = 2 - 7$ with particle-hole symmetry and equivalent noninteracting bands. While these results will be numerically identical to VDAT at $\mathcal{N} = 3$ with a G-type SPD, the 1RDMF offers extraordinary practical advantages. The computational cost of the 1RDMF can be broken into two parts. First, the interaction energy functional must be constructed for a given $N_{\rm orb}$ and J/U, and the computational cost is dominated by the solution of a collection of quantum spin models with $2N_{\rm orb}$ spins. Second, the total energy must be minimized for a given Hamiltonian by solving the saddle point equations for a and b, which has a minimal cost. For a fixed J/U and $N_{\rm orb}$, the interaction energy functional for arbitrary U can be obtained via scaling, allowing for the entire parameter space over U to be explored at a minimal computational cost. The total energy and the interaction energy are plotted as a function of U/t for $J/U = 0.05$ and $N_{\rm orb} = 2, 3, 5, 7$ (see Fig. 4). The dotted lines indicate a metastable metal or insulating phase. The Mott transition can be identified as a kink in the total energy or a discontinuity in the interaction energy, which is first-order in this case, consistent with previous Gutzwiller [58], slave boson [59], and DMFT [60] studies. Corresponding results for $J/U = 0, 0.25$ are provided in Ref. [41]. Additionally, we explore how the Mott transition value U_c depends on $N_{\rm orb}$ for many different values of J/U (see Fig. 5). For $J/U = 0$, we exactly recover the result from our previous VDAT study [40], which demonstrated excellent agreement with numerically exact DMFT solutions. For small J/U, the U_c increases with $N_{\rm orb}$, while the opposite happens for sufficiently large J/U. While previous DMFT studies already elucidated the fact that increasing J/U decreases U_c at a given $N_{\rm orb}$ for $N_{\rm orb} \leqslant 3$ [60–63], our results provide a clear understanding of how U_c depends on $N_{\rm orb}$ for a given J/U up to $N_{\rm orb} = 7$.

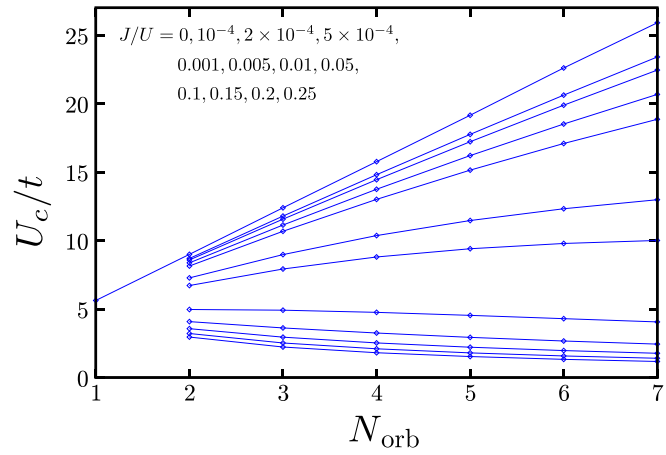

FIG. 5. Plot of U_c for the multiorbital Hubbard model on the Bethe lattice in $d = \infty$ as a function of $N_{\rm orb}$ for various J/U, where U_c monotonically decreases with increasing J/U for a given $N_{\rm orb}$.

In conclusion, we have provided a practical formalism for exactly executing the constrained search within the G-type $\mathcal{N} = 3$ SPD in $d = \infty$ to construct the 1RDMF for the multiorbital Hubbard model. We explicitly illustrate that there is nonanalyticity in the interaction energy functional for the multiorbital Hubbard model which gives rise to the Mott transition and properly describes the order of the transition. While the Mott transition in $d = \infty$ has been intensively studied, the 1RDMF demonstrates the universality of the Mott transition independent of the details of the band structure. Moreover, the 1RDMF is an efficient tool for accurately solving the ground-state properties of the multiorbital Hubbard model, yielding solutions for large N_{orb} which cannot be obtained by competing methods.

This work was supported by the INL Laboratory Directed Research & Development (LDRD) Program under DOE Idaho Operations Office Contract No. DE-AC07-05ID14517. This research used resources of the National Energy Research Scientific Computing Center, a DOE Office of Science User Facility supported by the Office of Science of the U.S. Department of Energy under Contract No. DE-AC02-05CH11231.

Data availability. The data that support the findings of this article are openly available [64].

[1] R. A. Donnelly and R. G. Parr, Elementary properties of an energy functional of first-order reduced density matrix, J. Chem. Phys. **69**, 4431 (1978).

[2] T. L. Gilbert, Hohenberg-Kohn theorem for nonlocal external potentials, Phys. Rev. B **12**, 2111 (1975).

[3] M. Levy, Universal variational functionals of electron-densities, 1st-order density-matrices, and natural spin-orbitals and solution of the *v*-representability problem, Proc. Natl. Acad. Sci. USA **76**, 6062 (1979).

[4] K. Pernal and K. J. H. Giesbertz, Reduced density matrix functional theory (RDMFT) and linear response time-dependent RDMFT (TD-RDMFT), in *Density-Functional Methods for Excited States*, edited by Nicolas Ferre, Michael Filatov, and Miquel Huix-Rotllant (Springer International Publishing, Cham, Switzerland, 2016), Vol. 368, p. 125.

[5] M. Piris, Exploring the potential of natural orbital functionals, Chem. Sci. **15**, 17284 (2024).

[6] M. Piris, Natural orbital functional theory, in *Reduced-Density-Matrix Mechanics: with Application to Many-Electron Atoms and Molecules*, edited by D. A. Mazziotti (John Wiley & Sons, New York, NY, 2007), Vol. 134, p. 387.

[7] E. Engel and R. M. Dreizler, *Density Functional Theory—An Advanced Course* (Springer, Berlin, 2011).

[8] J. Cioslowski, K. Pernal, and M. Buchowiecki, Approximate one-matrix functionals for the electron-electron repulsion energy from geminal theories, J. Chem. Phys. **119**, 6443 (2003).

[9] W. Kutzelnigg, Direct determination of natural orbitals natural expansion coefficients of many-electron wavefunctions.I. Natural orbitals in geminal product approximation, J. Chem. Phys. **40**, 3640 (1964).

[10] J. F. H. Lew-Yee, J. M. del Campo, and M. Piris, Advancing natural orbital functional calculations through deep learning-inspired techniques for large-scale strongly correlated electron systems, Phys. Rev. Lett. **134**, 206401 (2025).

[11] K. Pernal, The equivalence of the Piris natural orbital functional 5 (PNOF5) and the antisymmetrized product of strongly orthogonal geminal theory, Comput. Theor. Chem. **1003**, 127, (2013).

[12] M. Piris, X. Lopez, F. Ruiperez, J. M. Matxain, and J. M. Ugalde, A natural orbital functional for multiconfigurational states, J. Chem. Phys. **134**, 164102 (2011).

[13] M. Piris and J. M. Ugalde, Perspective on natural orbital functional theory, Int. J. Quantum Chem. **114**, 1169 (2014).

[14] R. Schade, E. Kamil, and P. Blochl, Reduced density-matrix functionals from many-particle theory, Eur. Phys. J. Spec. Top. **226**, 2677 (2017).

[15] E. Kamil, R. Schade, T. Pruschke, and P. E. Blochl, Reduced density-matrix functionals applied to the Hubbard dimer, Phys. Rev. B **93**, 085141 (2016).

[16] J. F. H. Lew-Yee and M. Piris, Metal-insulator transition described by NOFT, Rev. Cubana Fis. **42**, 30 (2025).

[17] R. Lopez-Sandoval and G. M. Pastor, Density-matrix functional theory of the Hubbard model: An exact numerical study, Phys. Rev. B **61**, 1764 (2000).

[18] R. Lopez-Sandoval and G. M. Pastor, Density-matrix functional theory of strongly correlated lattice fermions, Phys. Rev. B **66**, 155118 (2002).

[19] R. Lopez-Sandoval and G. M. Pastor, Interaction-energy functional for lattice density functional theory: Applications to one-, two-, and three-dimensional Hubbard models, Phys. Rev. B **69**, 085101 (2004).

[20] I. Mitxelena and M. Piris, An efficient method for strongly correlated electrons in two-dimensions, J. Chem. Phys. **152**, 064108 (2020).

[21] I. Mitxelena, M. Piris, and M. Rodriguez-Mayorga, On the performance of natural orbital functional approximations in the Hubbard model, J. Phys.: Condens. Matter **29**, 425602 (2017).

[22] I. Mitxelena, M. Piris, and M. Rodriguez-Mayorga, Corrigendum: On the performance of natural orbital functional approximations in the Hubbard model (2017 J. Phys.: Condens. Matter 29 425602), J. Phys. Cond. Matter **30**, 089501 (2018).

[23] I. Mitxelena, M. Rodriguez-mayorga, and M. Piris, Phase dilemma in natural orbital functional theory from the n-representability perspective, Eur. Phys. J. B **91**, 109 (2018).

[24] I. Mitxelena and M. Piris, An efficient method for strongly correlated electrons in one dimension, J. Phys.: Condens. Matter **32**, 17LT01 (2020).

[25] M. Saubanere, M. B. Lepetit, and G. M. Pastor, Interaction-energy functional of the Hubbard model: Local formulation and application to low-dimensional lattices, Phys. Rev. B **94**, 045102 (2016).

[26] M. Saubanere and G. M. Pastor, Density-matrix functional study of the Hubbard model on one- and two-dimensional bipartite lattices, Phys. Rev. B **84**, 035111 (2011).

[27] W. Tows, M. Saubanere, and G. M. Pastor, Density-matrix functional theory of strongly correlated fermions on lattice models

and minimal-basis Hamiltonians, Theor. Chem. Acc. **133**, 1422 (2014).
[28] N. Helbig, N. N. Lathiotakis, M. Albrecht, and E. Gross, Discontinuity of the chemical potential in reduced-density-matrix-functional theory, Europhys. Lett. **77**, 67003 (2007).
[29] N. N. Lathiotakis, S. Sharma, J. K. Dewhurst, F. G. Eich, M. Marques, and E. Gross, Density-matrix-power functional: Performance for finite systems and the homogeneous electron gas, Phys. Rev. A **79**, 040501(R) (2009).
[30] S. Sharma, J. K. Dewhurst, N. N. Lathiotakis, and E. Gross, Reduced density matrix functional for many-electron systems, Phys. Rev. B **78**, 201103(R) (2008).
[31] S. Sharma, J. K. Dewhurst, S. Shallcross, and E. Gross, Spectral density and metal-insulator phase transition in Mott insulators within reduced density matrix functional theory, Phys. Rev. Lett. **110**, 116403 (2013).
[32] Y. Shinohara, S. Sharma, J. K. Dewhurst, S. Shallcross, N. N. Lathiotakis, and E. Gross, Doping induced metal-insulator phase transition in NiO—A reduced density matrix functional theory perspective, New J. Phys. **17**, 093038 (2015).
[33] P. Kent and G. Kotliar, Toward a predictive theory of correlated materials, Science **361**, 348 (2018).
[34] A. Georges, G. Kotliar, W. Krauth, and M. J. Rozenberg, Dynamical mean-field theory of strongly correlated fermion systems and the limit of infinite dimensions, Rev. Mod. Phys. **68**, 13 (1996).
[35] G. Kotliar, S. Y. Savrasov, K. Haule, V. S. Oudovenko, O. Parcollet, and C. A. Marianetti, Electronic structure calculations with dynamical mean-field theory, Rev. Mod. Phys. **78**, 865 (2006).
[36] G. Kotliar and D. Vollhardt, Strongly correlated materials: Insights from dynamical mean-field theory, Phys. Today **57**(3), 53 (2004).
[37] Z. Cheng and C. A. Marianetti, Foundations of variational discrete action theory, Phys. Rev. B **103**, 195138 (2021).
[38] Z. Cheng and C. A. Marianetti, Variational discrete action theory, Phys. Rev. Lett. **126**, 206402 (2021).
[39] Z. Cheng and C. A. Marianetti, Precise ground state of multi-orbital Mott systems via the variational discrete action theory, Phys. Rev. B **106**, 205129 (2022).
[40] Z. Cheng and C. A. Marianetti, Gauge constrained algorithm of variational discrete action theory at N=3 for the multiorbital Hubbard model, Phys. Rev. B **108**, 035127 (2023).
[41] Z. Cheng and C. A. Marianetti, companion paper, Qubit parametrization of the variational discrete action theory for the multiorbital Hubbard model, Phys. Rev. B **113**, 085137 (2026).
[42] M. Chatzieleftheriou, A. Kowalski, M. Berovic, A. Amaricci, M. Capone, L. De Leoand, G. Sangiovanni, and L. de' Medici, Mott quantum critical points at finite doping, Phys. Rev. Lett. **130**, 066401 (2023).
[43] A. Muller, Explicit approximate relation between reduced 2-particle and one-particle density-matrices, Phys. Lett. A **105**, 446 (1984).
[44] G. Csanyi and T. A. Arias, Tensor product expansions for correlation in quantum many-body systems, Phys. Rev. B **61**, 7348 (2000).
[45] G. Csanyi, S. Goedecker, and T. A. Arias, Improved tensor-product expansions for the two-particle density matrix, Phys. Rev. A **65**, 032510 (2002).
[46] R. Zitko and T. Pruschke, Energy resolution and discretization artifacts in the numerical renormalization group, Phys. Rev. B **79**, 085106 (2009).
[47] M. Piris, Global method for electron correlation, Phys. Rev. Lett. **119**, 063002 (2017).
[48] R. Levy, M. A. Morales, and S. W. Zhang, Automatic order detection and restoration through systematically improvable variational wave functions, Phys. Rev. Res. **6**, 013237 (2024).
[49] H. Otsuka, Variational Monte-Carlo studies of the Hubbard-model in one-dimension and two-dimension—Off-diagonal intersite correlation-effects, J. Phys. Soc. Jpn. **61**, 1645 (1992).
[50] S. Sorella, Systematically improvable mean-field variational ansatz for strongly correlated systems: Application to the Hubbard model, Phys. Rev. B **107**, 115133 (2023).
[51] T. Yanagisawa, Crossover from weakly to strongly correlated regions in the two-dimensional Hubbard model off-diagonal wave function Monte Carlo studies of Hubbard model II, J. Phys. Soc. Jpn. **85**, 114707 (2016).
[52] T. Yanagisawa, Antiferromagnetism, superconductivity and phase diagram in the two-dimensional Hubbard model -off-diagonal wave function Monte Carlo studies of Hubbard model III—, J. Phys. Soc. Jpn. **88**, 054702 (2019).
[53] T. Yanagisawa, S. Koike, and K. Yamaji, Off-diagonal wave function Monte Carlo studies of Hubbard model I, J. Phys. Soc. Jpn. **67**, 3867 (1998).
[54] T. Yanagisawa, S. Koike, and K. Yamaji, Ground state of the three-band Hubbard model, Phys. Rev. B **64**, 184509 (2001).
[55] T. Yanagisawa, M. Miyazaki, and K. Yamaji, Ground-state phase diagram of the three-band d-p model, Europhys. Lett. **134**, 27004 (2021).
[56] Y. X. Chen, L. F. Zhang, E. Weinan, and R. Car, Hybrid auxiliary field quantum Monte Carlo for molecular systems, J. Chem. Theory Comput. **19**, 4484 (2023).
[57] J. P. Perdew, R. G. Parr, M. Levy, and J. L. Balduz, Density-functional theory for fractional particle number - Derivative discontinuities of the energy, Phys. Rev. Lett. **49**, 1691 (1982).
[58] J. Bunemann and W. Weber, Generalized Gutzwiller method for $n \geqslant 2$ correlated bands: First-order metal-insulator transitions, Phys. Rev. B **55**, 4011 (1997).
[59] H. Hasegawa, Slave-boson functional-integral approach to the Hubbard model with orbital degeneracy, J. Phys. Soc. Jpn. **66**, 1391 (1997).
[60] Y. Ono, M. Potthoff, and R. Bulla, Mott transitions in correlated electron systems with orbital degrees of freedom, Phys. Rev. B **67**, 035119 (2003).
[61] L. de' Medici, Hund's coupling and its key role in tuning multiorbital correlations, Phys. Rev. B **83**, 205112 (2011).
[62] J. E. Han, M. Jarrell, and D. L. Cox, Multiorbital Hubbard model in infinite dimensions: Quantum Monte Carlo calculation, Phys. Rev. B **58**, R4199(R) (1998).
[63] T. Pruschke and R. Bulla, Hund's coupling and the metal-insulator transition in the two-band Hubbard model, Eur. Phys. J. B **44**, 217 (2005).
[64] Z. Cheng, vdatqubithalf (2025), https://github.com/chengzhengqian/vdatqubithalf.